Stacked Approximated Regression Machine: A Simple Deep Learning Approach

Zhangyang Wang[†], **Shiyu Chang**[‡], **Qing Ling**[§], **Shuai Huang**[△],
Xia Hu[◇], **Honghui Shi**[†], **and Thomas S. Huang**[†]
† Beckman Institute, University of Illinois at Urbana-Champaign
‡ IBM T. J. Watson Research Center
§ Department of Automation, University of Science and Technology of China
△ Department of Industrial & Systems Engineering, University of Washington
◇ Department of Computer Science & Engineering, Texas A&M University
{zwang119, hshi10, t-huang1}@illinois.edu shiyu.chang@ibm.com
qingling@mail.ustc.edu.cn shuaih@uw.edu hu@cse.tamu.edu

Abstract

This paper proposes the Stacked Approximated Regression Machine (SARM), a novel, simple yet powerful deep learning (DL) baseline. We start by discussing the relationship between regularized regression models and feed-forward networks, with emphasis on the non-negative sparse coding and convolutional sparse coding models. We demonstrate how these models are naturally converted into a unified feed-forward network structure, which coincides with popular DL components. SARM is constructed by stacking multiple unfolded and truncated regression models. Compared to the PCANet, whose feature extraction layers are completely linear, SARM naturally introduces non-linearities, by embedding sparsity regularization. The parameters of SARM are easily obtained, by solving a series of light-weight problems, e.g., PCA or KSVD. Extensive experiments are conducted, which show that SARM outperforms the existing simple deep baseline, PCANet, and is on par with many state-of-the-art deep models, but with much lower computational loads.

1 Motivation and Overview

This work was directly motivated by PCANet [5], which was designed to be a simple but competitive deep learning (DL) baseline. Classical deep neural networks (DNNs) [18] consist of stacked trainable stages, followed by a supervised loss. Each stage comprises a fully-connected or convolutional layer together with a nonlinear neuron function, and optionally with a feature pooling layer. Despite the remarkable performance breakthrough [24, 11], DNNs usually rely on time-consuming training by back propagation (BP), careful hyper-parameter tuning, and other empirical tricks [26].

In contrast, a PCANet comprises only very basic data processing components. A cascaded principal component analysis (PCA) is employed to learn multi-stage filter banks. There is no nonlinear operation involved until its very last layer, where binary hashing and histograms are conducted to compute the output features. Thus, this architecture can be learned in an efficient manner. The authors in [5] discovered the surprising fact, that a naive PCANet could compete with the state-of-the-art DNNs in a wide range of recognition and classification tasks. PCANet thus serves as a good baseline to empirically justify the usage of more sophisticated processing components for deep networks.

Our goal is to design a novel DL baseline, which demonstrates more competitive performance in discriminative tasks, but remains as an easily trainable model as PCANet. We construct a feed-forward feature learning hierarchy, by stacking truncated and regularized regression-type models, called *Stacked Approximated Regression Machine* (**SARM**). The architectures of many existing deep

29th Conference on Neural Information Processing Systems (NIPS 2016), Barcelona, Spain.

models [18, 24, 11] can be shown as special cases of SARM. Solving the parameters of SARM requires no BP; instead, they could be obtained by solving a series of light-weight problems, such as PCA or KSVD [7]. Compared to PCANet, whose feature extraction layers (stacked PCA filters) are completely linear, SARM naturally introduces non-linearities by enforcing sparsity regularization as a prior, which has been found to benefit discriminative tasks [6]. As shown in our study, SARM gains consistent performance advantages over PCANet. Further, SARM is on par with, sometimes even outperforms many state-of-the-art DNNs, with much lower computational loads. It proves to serve as a competitive baseline to many DL tasks. The derivation of SARM also provides instructive information on interpreting the working mechanism of deep networks.

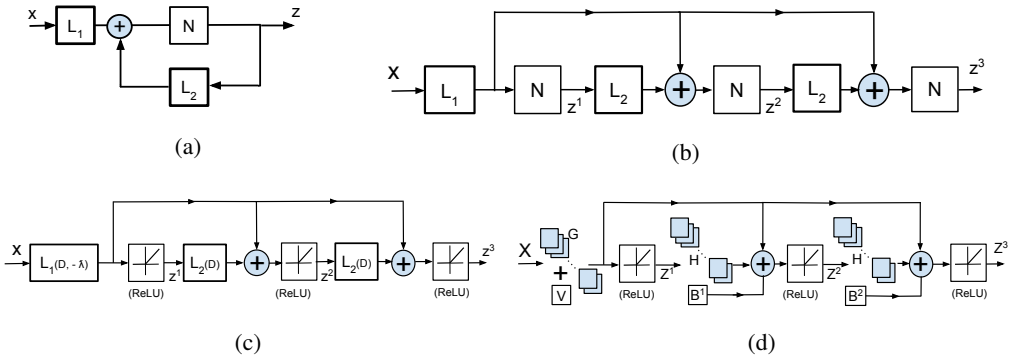

Figure 1: (a) The recursive system diagram for Eqn. (2); (b) A 2-iteration ARM, unfolded and truncated from (a); (c) A 2-iteration n-ℓ_1-ARM; (d) A 2-iteration n-conv-ℓ_1-ARM.

2 Related Work

In addition to PCANet, the framework of SARM is related to, but substantially different from, the following prior work:

- *Autoencoder (AE) and Predictive Sparse Decomposition (PSD).* (Stacked) AE and its variants were mostly studied for pre-training deep models [2, 22]. PSD [14, 17], as a variant of AE, learns efficient feed-forward filter banks and produces sparse features. However, PSD has to train the desired sparse encoder (regressor), jointly with the decoder (dictionary) and the sparse code. It thus leads to entangled variables and more complicated optimizations. In comparison, SARM greatly alleviates the computational complexity by solving the encoder parameters directly.
- *Wavelet Scattering Network (ScatNet).* Different from typical CNNs, ScatNet [4] stacks wavelet operators as the convolutional filters, without any learning. Such a multi-stage architecture with pre-fixed filter bank has demonstrated superior performance over DNNs, and has found clear mathematical justifications. However, as argued by [5], ScatNet is less capable for tasks such as face recognition, where the intra-class samples include significant amount of illumination changes and occlusions.
- *Deep Network Implementation of Sparse Coding.* There has been a blooming interest in bridging sparse coding (sparsity-regularized linear regression) and DL models. [8, 29, 28, 27] leveraged similar ideas on fast trainable regressors, and constructed feed-forward network approximations to solve the sparse coding (i.e., sparsity-regularized linear regression) models. Lately, [33] demonstrated both theoretically and empirically that a trained deep network is potentially able to recover ℓ_0-based sparse representations.

3 Approximated Regression Machine

We start from the following *regularized regression* form, which represents a large family of feature learning models, such as PCA and sparse coding [7]:

$$\mathbf{a} = \arg\min_{\mathbf{a}} \tfrac{1}{2}||\mathbf{x} - \Phi(\mathbf{D}, \mathbf{a})||_F^2 + \Psi(\mathbf{a}). \tag{1}$$

Here $\mathbf{x} \in R^n$ denotes the input data, $\mathbf{a} \in R^m$ is the feature to learn, and $\mathbf{D} \in R^{n \times m}$ is the representation basis. $\Phi(\mathbf{D}, \mathbf{a})$: $R^{n \times m} \times R^m \rightarrow R^n$ defines the form of feature representation. The regularization term $\Psi(\mathbf{a})$: $R^m \rightarrow R$ further incorporates the problem-specific prior knowledge. Not surprisingly, many instances of Eqn. (1) could be solved by a similar class of iterative algorithms:

$$\mathbf{z}^{k+1} = \mathcal{N}(\mathcal{L}_1(\mathbf{x}) + \mathcal{L}_2(\mathbf{z}^k)), \tag{2}$$

where $\mathbf{z}^k \in R^m$ denotes the intermediate output of the k-th iteration, k = 0, 1, $\cdots$. $\mathcal{L}_1$ and $\mathcal{L}_2$ are linear (or convolutional) operators, while $\mathcal{N}$ is a simple non-linear operator. Eqn. (2) could be expressed by the recursive system in Fig. 1 (a), whose fixed point is expected to be the solution $\mathbf{a}$ of Eqn. (1). Furthermore, the recursive system in Fig. 1 (a) could be *unfolded* and *truncated* to k iterations, to construct a (k+1)-layer feed-forward network. Without any further tuning, the resulting architecture will output a k-iteration approximation of the exact solution $\mathbf{a}$. We name it as the k-iteration *Approximated Regression Machine* (**ARM**), which is illustrated in Fig. 1 (b) (we set k = 2 for illustration purpose).

A popular instance of Eqn. (1), the sparse coding model [7], corresponds to $\Psi(\mathbf{a}) = \lambda||\mathbf{a}||_1$, $\Phi(\mathbf{D}, \mathbf{a}) = \mathbf{D}\mathbf{a}$, with $||\mathbf{D}||_2$ = 1 by default. Then, the concrete function forms are given as ($\mathbf{u}$ is a vector and u_i is its i-th element):

$$\mathcal{L}_1(\mathbf{x}) = \mathbf{D}^T\mathbf{x},\ \mathcal{L}_2(\mathbf{z}^k) = (\mathbf{I} - \mathbf{D}^T\mathbf{D})\mathbf{z}^k,\ \mathcal{N}(\mathbf{u})_i = \text{sign}(u_i)(|u_i| - \lambda)_+, \tag{3}$$

where $\mathcal{N}$ is an element-wise soft shrinkage function. The unfolded and truncated version of Eqn. (3) was first proposed in [8], called the learned iterative shrinkage and thresholding algorithm (LISTA). Alternatively, it could be viewed as an ARM regularized by ℓ_1 norm, denoted by ℓ_1-ARM for short.

Many recent works [8, 25, 29] followed LISTA and developed various models, all of which might be treated as ARMs as well. In this paper, we focus on the sparsity regularization to adapt ARM for discriminative tasks [6]. Without loss of generality, our model and conclusion could be extended to other tasks as well. We derive two useful variants: 1) n-ℓ_1-ARM, based on *non-negative sparse coding* [34], and 2) n-conv-ℓ_1-ARM, based on *non-negative convolutional sparse coding* [32]. Enforcing non-negativity was shown to be helpful in many visual recognition tasks [34]. What is more, it allows $\mathcal{N}$ to bear the identical form as the standard neuron(s), and facilitates our interpretation and comparison with existing deep networks. Recall that, ARM is amenable to various prior knowledge beyond sparsity, such as the ℓ_∞-regularization discussed in [30].

Non-negative ℓ_1-ARM By enforcing $\Psi(\mathbf{a}) = \lambda||\mathbf{a}||_1$, $\mathbf{a} \geq 0$, and $\Phi(\mathbf{D}, \mathbf{a}) = \mathbf{D}\mathbf{a}$, $||\mathbf{D}||_2$ = 1, Eqn. (2) could be adapted to solve the non-negative sparse coding problem:

$$\mathcal{L}_1(\mathbf{x}) = \mathbf{D}^T\mathbf{x} - \lambda,\ \mathcal{L}_2(\mathbf{z}^k) = (\mathbf{I} - \mathbf{D}^T\mathbf{D})\mathbf{z}^k,\ \mathcal{N}(\mathbf{u})_i = \max(u_i, 0). \tag{4}$$

A by-product of applying non-negativity is that the original sparsity coefficient λ now occurs in $\mathcal{L}_1$ as the bias term of this layer, rather than appearing in $\mathcal{N}$ as in Eqn. (3). As a result, $\mathcal{N}$ in Eqn. (4) now has exactly the same form as the popular neuron of Rectified Linear Unit (ReLU) [18]. Eqn. (4) could be converted to a non-negative ℓ_1-ARM (n-ℓ_1-ARM). The architecture of k-iteration n-ℓ_1-ARM is plotted in Fig. 1 (c), where k = 2.

Non-negative convolutional ℓ_1-ARM When handling natural images, the linear sparse coding models have to partition an image into patches with spatial inconsistency. In contrast to linear combinations, convolutional sparse coding (CSC) [32] represents an entire image as the summation of convolutions of the feature maps and the corresponding filters. Assume $\mathbf{X} \in R^{M \times N}$ is an input image, $\mathcal{F} = \{\mathcal{F}_i\}$, $i = 1, 2, \cdots, c$, is a group of $s \times s$ filters, and $\mathbf{Z} = \{\mathbf{Z}_i\}$ are the feature maps corresponding to $\{\mathcal{F}_i\}$. We take $\Psi(\mathbf{Z}) = \lambda \sum_{i=1}^c ||\mathbf{Z}_i||_1$, $\mathbf{Z}_i \succeq \mathbf{0}, \forall i$, and $\Phi(\mathcal{F}, \mathbf{Z}) = \sum_{i=1}^c \mathcal{F}_i * \mathbf{Z}_i$.

Following the alternating direction method of multipliers (ADMM) [32], we denote $\mathbf{U}^k = \{\mathbf{U}_i^k\}$ ($i = 1, 2, \ldots, c$) as the set of Lagrange multipliers; ρ is a positive constant (with a default value of 0.6); and $\mathscr{F}^{-1}$ is the inverse Fourier transform. Same as in [32], we further define $\hat{\mathcal{F}}_i$ as the DFT domain convolution operator of $\mathcal{F}_i$, as well as $\mathbf{F} = \{\hat{\mathcal{F}}_i\}$, ($i = 1, 2, \ldots, c$). Eventually, we obtain the iterative formula (2) for solving non-negative CSC ($\mathbf{Z}^{k+1} \in R^{M \times N}$ is the intermediate variable):

$$\begin{aligned}
&\mathcal{L}_1(\mathbf{X}) = \mathbf{G} * \mathbf{X} + \mathbf{V},\ \mathcal{L}_2(\mathbf{Z}^k) = \mathbf{H} * \mathbf{Z}^k + \mathbf{B}^k,\ \mathcal{N}(\mathbf{u})_i = \max(u_i, 0), \text{where} \\
&\mathbf{G} = \mathscr{F}^{-1}\{(\mathbf{F}^H\mathbf{F} + \rho I)^{-1}\mathbf{F}^H\}, \quad \mathbf{V} = -\lambda/\rho, \\
&\mathbf{H} = \rho\mathscr{F}^{-1}\{(\mathbf{F}^H\mathbf{F} + \rho I)^{-1}\}, \quad \mathbf{B}^k = \mathbf{U}^k/\rho - \mathscr{F}^{-1}\{(\mathbf{F}^H\mathbf{F} + \rho I)^{-1}\} * \mathbf{U}^k.
\end{aligned} \tag{5}$$

Eqn. (5) could also be unfolded and truncated to k iterations, leading to a non-negative convolutional ℓ_1-ARM (n-conv-ℓ_1-ARM), as illustrated in Fig. 1 (d) , where k = 2. In addition to being fully convolutional (while n-ℓ_1-ARM is fully-connected), one may notice the new bias term $\mathbf{B}^k$ in $\mathcal{L}_2$. It depends on the Lagrange multipliers $\mathbf{U}^k$, and is updated throughout iterations.

Important special case: 0-iteration ARM We first make an aggressive approximation of Eqn. (4), by setting k = 0 and assuming $\mathbf{z}^0 = 0$, we have:

$$\mathbf{z} = \mathcal{N}(\mathbf{D}^T\mathbf{x} - \lambda). \tag{6}$$

Note that even a nonzero $\mathbf{z}^0$ is assumed, it could be absorbed into the bias term $-\lambda$. Eqn. (6) is exactly a fully-connected layer followed by ReLU neurons, one of the most standard building blocks in existing deep models. Similarly, (5) could be also simplified with k = 0 as:

$$\mathbf{Z} = \mathcal{N}(\mathbf{G} * \mathbf{X} + \mathbf{V}), \text{where } \mathbf{G} = \mathscr{F}^{-1}\{(\mathbf{F}^H\mathbf{F} + \rho I)^{-1}\mathbf{F}^H\},\ \mathbf{V} = -\lambda/\rho. \tag{7}$$

Eqn. (7) removes the hassle of Lagrange multipliers, and is reduced to the classical form of a convolutional layer followed by ReLU neurons.

There are other 0-iteration ARMs that become a linear or convolutional layer plus special neurons [29, 30]. One exception occurs in the ℓ_0-constrained regression defined in [29]: its corresponding 0-iteration ARM will lead to a layer plus a max-pooling operator.

4 Stacked Approximated Regression Machine

While a k-iteration ARM (k > 0) is a multi-layer network by itself, the parameters of $\mathcal{L}_1$ and $\mathcal{L}_2$ are not independent. For example, they both hinge on $\mathbf{D}$ in Eqn. (3). Furthermore, $\mathcal{L}_2$ recurs k times with the identical parameters. Therefore, the actual modeling power of an ARM is limited. Fortunately, this disadvantage can be overcome, by stacking p ARMs, each of which has $k = d_i$ iterations, $i = 1, 2, \cdots, p$. The resulting hierarchical model, termed the *Stacked Approximated Regression Machine* (**SARM**), is a feed-forward network with depth $p + \sum_i^p d_i$. Classifiers are to be trained on the output features of SARM.

Compared to PCANet, whose feature extraction layers (stacked PCA filters) are completely **linear**, SARM naturally introduces **non-linear** mappings, by enforcing sparsity regularization in each ARM as a prior, which has been found to benefit classification and other discriminative tasks [6]. It is obvious to see that many conventional deep feed-forward networks such as [18, 24] are special cases of SARM. They are predominantly alternating stacks of trainable layers (either fully-connected or convolutional), and nonlinearities (e.g., ReLU). Assuming no shared weights, from the SARM viewpoint, such networks could be decomposed into a series of either 0-iteration n-conv-ℓ_1-ARMs, or 0-iteration n-ℓ_1-ARMs, i.e., d_i = 0, $\forall i$. Each ARM is "roughly" solving a non-negative sparse coding or CSC model in essence, w.r.t. its own independent dictionary or filter bank. The output for each ARM is a one-step (i.e., k = 0) truncated approximation of the "ground-truth" sparse code or feature maps, which is then fed into the subsequent ARM as its input. For a fair experimental comparison with existing deep models, we hereinafter focus our further discussion on SARMs composed of only n-conv-ℓ_1-ARMs and n-ℓ_1-ARMs.

Resemblance to residual learning? When d_i > 0, $\exists i$, the skip connections of the corresponding ARM are preserved as inter-layer "shortcuts" in SARM. That is reminiscent of the recent residual learning strategy [11, 12], which illustrates the power of shortcuts connecting hidden layers.

In Fig. 2, we compare a 2-iteration ARM, with a 3-layer network composed of one layer (W_1) followed by a two-layer residual learning module (W_2, W_3). The ARM shortcut interconnects the outputs of every single layer ($\mathcal{L}_1$, and two $\mathcal{L}_2$s), whereas the residual learning shortcut skips intermediate layers. It is also noteworthy that the skipped weights W_2, W_3 (Fig. 2 (b)) are not tied, while the $\mathcal{L}_2$ layers are supposed to share weights (Fig. 2 (a)).

Furthermore, the original deep residual network is designed to be a stack of the 2-layer residual learning modules in Fig. 2 (b), without a separate layer like W_1 (see Fig. 1 (b) in [12]). Hence, SARM does not directly lead to the construction of deep residual networks. However, their intriguing structural resemblance will be investigated further in our future work.

Compatibility with other DL techniques It is very straightforward to incorporate other activation functions into SARM. For others piecewise linear shrinkage-type neurons, such as leaky ReLU and

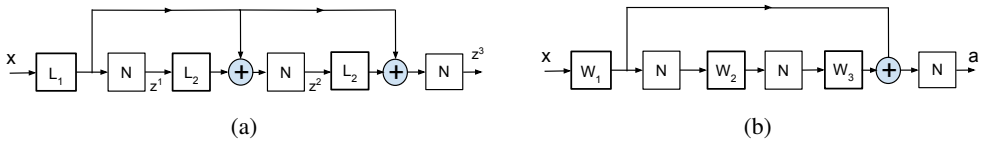

(a) (b)

Figure 2: Comparison between: (a) A 3-layer network, formed by a 2-iteration ARM; (b) A 3-layer network, with a 2-layer residual learning module, where W_i (i = 1, 2, 3) denotes the layer weights and batch normalization [13] is omitted.

PReLU [10]), they could be obtained by converting (adaptively) reweighted sparse coding models to ARMs, given properly defined weights. We also noticed that the "kernelized" counterparts of ARMs can result in more complicated nonlinear neurons, and will discuss them in future work.

Popular training and regularization techniques, such as batch normalization [13], dropout [18] and max pooling, could be easily inserted into SARM as "accessory" building blocks. Despite possible benefits to performance, they will not affect how SARM constructs a deep model, i.e., hierarchically mapping DNN trainable layers and inferring the parameters from regularized regression models. For example, max pooling is applied to SARM in Section 5.3.

Remarks on the interpretability of DL From the derivation of SARM, many existing deep models [18, 24, 11] could be interpreted as the hierarchical sparsifying process [31], with regard to a series of different dictionaries/filter banks. It thus generates more sparse, abstract features in higher layers [15]. We may learn more instructive information about the mechanism of general deep networks. For instance, Eqns. (4) and (5) establish the equivalence between ReLU and the shrinkage operator for non-negative sparse coding/CSC. Note that those are well-known to be effective in extracting semantically meaningful visual information [34]. Taking the layer-wise bias as another example: in Eqns. (6) or (7), adjusting the bias term corresponds to tuning the weight of the sparsity regularization.

4.1 Obtaining SARM Parameters

The parameters of the entire SARM are solved recursively. The current ARM's parameters are calculated using the output from the previous ARM. Then, the output of the current ARM is fed into the subsequent ARM (or the classifier, if the current one is the last ARM), as its input. In Eqn. (4), the parameters of $\mathcal{L}_1$ and $\mathcal{L}_2$ depend on the dictionary $\mathbf{D}$. Since Eqn. (4) is inspired by solving sparse coding models, it is natural to compute $\mathbf{D}$ using the classical KSVD algorithm [7]. In Eqn. (5), we choose $\mathcal{F}$ to be the c leading principal eigenvectors of the input data matrix (please refer to [5] for more details in constructing "PCA filters"). λ in both Eqns. (4) and (5) could be chosen either empirically, or by cross-validations.

If $\forall i$, $d_i = 0$, then only $\mathcal{L}_1$ or $\mathcal{G}$ needs to be computed based on the fixed $\mathbf{D}$ or $\mathcal{F}$. If $\exists i$, $d_i > 0$, $\mathbf{D}$ or $\mathcal{F}$ could be re-used to compute $\mathcal{L}_2$ or $\mathbf{H}$. For n-conv-ℓ_1-ARM, if $d_i > 0$, we also record the values of $\mathbf{U}^k$ over iterations while solving Eqn. (5) by ADMM, in order to estimate $\mathbf{B}^k$, $k = 1, 2, \cdots, d_i$.

Two Variants: SARM-s and SARM-r Inspired by [5], we could construct two variants of SARM, which differ in the way of obtaining parameters. For classification tasks, we may enhance the supervision of the learned filters, by incorporating class labels during training. To obtain $\mathcal{F}$, we solve the filters by multi-class linear discriminant analysis (LDA) instead of PCA, following the identical procedure suggested by [5]. As for $\mathbf{D}$, we replace KSVD with the label-consistent KSVD algorithm [16]. We call such networks as *SAMR-s*.

We may further eliminate the necessity of training data, and replace the SARM parameters with random matrices/filters of the same dimensionality, whose elements are generated from the standard Gaussian distribution. Such networks are denoted as *SAMR-r*.

4.2 Training Complexity

To see how light the training complexity of SARM is, let us look at its two major building blocks discussed above. For k-iteration n-ℓ_1-ARM, the computational complexity consists of three parts:

- *Computing* $\mathbf{D}$: Given T input samples $\in R^n$, and assuming that KSVD is adopted, the computational complexity for $\mathbf{D} \in R^{n\times m}$ is $\mathcal{O}(QT(K^2m + 2mn))$, where K is the desired sparsity of $\mathbf{a} \in R^m$. Q absorbs iteration numbers of the batch orthogonal matching pursuit [23]. If $K \ll m, n$ holds, the complexity of this part is $\mathcal{O}(QTmn)$.
- *Constructing the parameters of* $\mathcal{L}_1$*, and* $\mathcal{L}_2$: $\mathcal{L}_1$ simply takes a transpose of $\mathbf{D}$. $\mathcal{L}_2$ is handled only if $k > 0$, and the complexity of matrix multiplication is $\mathbf{D}^T\mathbf{D} = \mathcal{O}(m^2n)$.
- *Calculating the output of ARM*: The last step is to pass T samples through the current trained ARM, whose output is fed into the next ARM. These matrix multiplications have the total complexity of $\mathcal{O}(T(mn + km^2))$.

In summary, the overall training complexity of k-iteration n-ℓ_1-ARM is $\mathcal{O}(QTmn)$ if $k = 0$, and $\mathcal{O}(QTmn+m^2n+Tkm^2)$ if $k > 0$. As a comparison, when using AE to (pre-)train a fully-connected layer $\in R^{m\times n}$ (same as 0-iteration n-ℓ_1-ARM), the complexity is $\mathcal{O}(Q'Tmn)$, where Q' absorbs iteration numbers in BP. However, it is a well-known empirical fact that $Q' \gg Q$.

For k-iteration n-conv-ℓ_1-ARM, the complexity is similarly divided into three parts. First, given T input samples $\in R^{M\times N}$, c PCA filters are obtained with the complexity $\mathcal{O}(TMNs^4)$, which is dominated by the matrix inner-product step [5]. Then, the computational loads of $\mathbf{G}$ and $\mathbf{H}$ are dominated by solving $(\mathbf{F}^H\mathbf{F} + \rho I)^{-1}$, whose complexity is $\mathcal{O}(MNc^3)$ (see (25) in [3]). Finally, it takes $\mathcal{O}(kTMNcs^2)$ to calculate the output. The overall training complexity of k-iteration n-conv-ℓ_1-ARM is hence $\mathcal{O}((c^3 + kTs^2c + Ts^4)MN)$. Note that in practice, $c < M, N$, and $s \ll M, N$.

5 Experiments

5.1 Comparison Experiments in Visual Recognition

5.1.1 Face Recognition on MultiPIE Dataset

We first focus on the problem of face recognition with one gallery image per person, and use part of MultiPIE [9] as the generic faces training set. MultiPIE contains 337 subjects across simultaneous variations in pose, expression, and illumination. We select the images of 129 subjects that enrolls all the four sessions as the training data. The remaining 120 new subjects in Session 1 are used for gallery training and testing. Frontal view of each subject with neutral expression and frontal illumination is used in gallery, and the rest for testing. We classify all the possible variations into 7 test sets, namely cross illumination, cross expression, cross pose, cross expression-plus-pose, cross illumination-plus-expression, cross illumination-plus-pose, and cross illumination-plus-expression-and-pose. All other details are identical to [5].

While PCANet and its variants are designed only to be convolutional, SARM is completely suitable to fully-connected, fully convolutional, or even mixed structures. We compare an extensive variety of **14** methods, divided into three groups:

- *Group 0: hand-crafted features* including: 1) Gabor features [20]; and 2) local binary patterns (LBP) [1].
- *Group 1: fully-connected models* including: 1) Stacked AE; and 2) SARM consisting of 0-iteration n-ℓ_1-ARMs. Further, as discussed in Section 3.1, the parameters of such a fully-connected SARM could be solved by KSVD, label-consistent KSVD, or random matrices, denoted as SARM-fc, SARM-fc-s and SARM-fc-r, respectively.
- *Group 2: fully convolutional models* including: 1) fully convolutional networks (FCN) [21]; 2) ScatNet [4]; 3) PCANet, LDANet, and RandNet [5]; 4) SARM consisting of 0-iteration n-conv-ℓ_1-ARMs. Similar to the above, the filters could be obtained by PCA, LDA, or random filters, leading to SARM-conv, SARM-conv-s and SARM-conv-r, respectively.

We follow the convention in [5] to use 2-layer networks, for a proof of concept. We will later investigate deeper models for imagenet classification. For fully-connected models in group 1, we set both hidden layers to be of dimension 512. For ScatNet, the number of scales and the number of orientations are set to 3 and 8, respectively. For all else in group 2, we set the filter channel number c to be 8, with the filter size to be 5×5, for both layers. Each convolution layer is followed by 2×2 max-pooling. We follow [5] to use the nearest neighbor (NN) classifier with the chi-square distance

Table 1: Comparison of face recognition rates (%) of various methods on MultiPIE test sets (cross illumination = I; cross expression = E; cross pose = P).

Methods	Test Sets	I.	E	P	E+P	I+E	I+P	I+E+P
Group 0	Gabor [20]	68.75	94.17	84.17	64.70	38.09	39.76	25.92
	LBP [1]	79.77	98.33	95.63	86.88	53.77	50.72	40.55
Group 1	Stacked AE	66.55	76.70	64.93	55.76	50.98	45.56	40.52
	SARM-fc	75.26	83.03	85.21	80.08	71.33	64.52	55.50
	SARM-fc-s	78.86	88.57	86.03	81.42	71.07	64.76	54.55
	SARM-fc -r	55.79	58.42	55.25	46.40	45.21	33.38	30.71
Group 2	FCN [21]	42.47	70.52	70.06	52.33	22.08	22.91	16.77
	ScatNet [4]	20.88	66.67	71.46	54.37	14.51	15.00	14.47
	PCANet [5]	**100.00**	99.17	93.33	87.29	87.89	75.29	**66.49**
	LDANet [5]	96.02	99.17	93.33	83.96	65.78	60.14	46.72
	RandNet [5]	97.64	97.50	83.13	75.21	63.87	53.50	42.47
	SARM-conv	99.24	99.50	96.93	85.26	70.86	65.54	52.46
	SARM-conv-s	**100.00**	**99.56**	**97.03**	**90.25**	**88.63**	**83.50**	64.67
	SARM-conv-r	92.82	93.56	85.76	75.31	67.77	55.51	43.74

for RandNet, PCANet, LDANet and LBP, and with the cosine distance for Gabor and ScatNet. For other 8 methods, we use the softmax classifier: Stacked AE and FCN are jointly fine-tuned with the classifier, while others train the classifier on top of the extracted features. All network-type models use ReLU as the neuron. Dropout [18] is applied only to Stacked AE, and no batch normalization [13] is employed. All other details are configured identically as in Section 3.1.1.D of [5].

The performance of all methods is compared in Table 1. Not surprisingly, feature learning models show superior performance, especially the fully convolutional models. Particularly, SARM-conv-s wins on 5 out of 7 test sets, ties for the first place on the first set, and is the second best on the last set. We also notice that whenever illumination varies, the performance of hand-crafted features drops significantly. In contrast, SARM, PCANet, and their variants all seem to alleviate this drawback.

We further compare methods within the same group. In group 1, SARM-fc and SARM-fc-s outperform Stacked AE in all cases with large margins between 10% - 20%. Especially, SARM-fc-s is observed to take good advantage of discriminative information, and obtains superior performance to SARM-fc in most test sets. The performance of SARM-fc-r, although not as satisfactory as SARM-fc/SARM-fc-s, is still comparable to Gabor features on the last three challenging sets. In group 2, ScatNet and FNN do not perform well in this specific task, as observed also in [5]. Whereas the performance of LDANet is consistently inferior to that of PCANet, SARM-conv-s evidently benefits from the label information incorporated during training. It implies that the SARM models may embed supervised information in their parameters better, and are thus more suitable for discriminative tasks. Another interesting observation is that both RandNet and SARM-conv-r generate remarkable results. Both of them outperform Gabor feature in all 7 test sets, and even LBP on 4 of them. Their performance is especially impressive, considering the minimum efforts needed to obtain their parameters.

5.1.2 Digit Recognition on MNIST Datasets

We then evaluate all the methods in groups 1 and 2 using the standard MNIST dataset [19]. All models are configured the same as in MultiPIE, except that we enlarge the filter size to be 7×7 for convolutional models. No data augmentation is performed. The testing error rates of the various methods on MNIST are shown in Table 2. While both SARM-conv-s and ScatNet produce the best results[1], we observe that SARM-conv and SARM-conv-r also generate comparable performance.

5.2 A SARM Baseline to Imagenet Classification

We try our proposed SARM framework for the image classification task on the ILSVRC-2012 dataset, which serves as a baseline to the VGGnet [24]. The dataset includes 1000 classes of images. We adopt the training set of 1.3M images, and follow [24] to use the set of 50K images for testing. We

[1]Note in [4], the lowest error rate of ScatNet on MNIST was reported to be 0.43%, with an SVM classifier using RBF kernels.To seek a fair comparison, we re-train a softmax classifier on the output features of ScatNet.

Table 2: Comparison of error rates (%) of the various methods on the MNIST dataset.

Method	SAE	SARM-fc	SARM-fc-s	SARM-fc-r	FNN	ScatNet
Accuracy	3.03	1.57	1.52	1.70	0.53	0.46
Method	PCANet	LDANet	RandNet	SARM-conv	SARM-conv-s	SARM-conv-r
Accuracy	0.69	0.62	0.63	0.47	0.46	0.49

follow the single-scale (256) training, and conduct both single-scale (256) and multi-scale (224, 256, 288) testing. The classification performance is evaluated using both the top-1 and top-5 errors. Two configurations, VGG-16 and VGG-19 (i.e., models D and E in [24]), are evaluated. VGG-16 has 16 convolutional layers followed by 3 fully-connected layers, while VGG-19 has 3 more convolutional layers. ReLU neurons and max pooling are utilized.

We use 0-iteration n-ℓ_1-ARMs and n-conv-ℓ_1-ARMs, to construct two SARM models, whose architectures are identical to VGG-16 and VGG-19, respectively. We evaluate both SARM and SARM-s cases, while leaving out SARM-r as its performance is mostly inferior. During experiments, when the inputs are RGB images, we first convert them to the YUV format, then train three groups of 2-D filters independently, on the Y, U and V channel images, respectively. We then combine the learned groups of filters to 3-D cubes, and finally convert them back to 3-D filters that are applicable to the RGB domain. The simplified approach makes our pre-training more affordable. All other training details are carefully set to be identical with the original models [18, 24].

Interestingly, we observe that each ARM's parameters could be reliably obtained, using a tiny portion of the training data. In our experiments, instead of running through the entire training set, we draw an small i.i.d. subset (as low as 0.5% of the training set), to solve the parameters for each ARM. That could save much computation and memory.

Table 3: Top-1 and top-5 classification errors (%) on the ILSVRC-2012 dataset, with: 1) original VGGnet [24]; 2) SARM; 3) SARM-s; 4) SARM-s jointly tuned with the classifier (**ss** = single-scale testing; **ms** = multi-scale testing).

	VGG-16 (ss)		**VGG-19 (ss)**		**VGG-16 (ms)**		**VGG-19 (ms)**	
Method	**Top-1**	**Top-5**	**Top-1**	**Top-5**	**Top-1**	**Top-5**	**Top-1**	**Top-5**
original	27.03	8.82	**27.35**	9.01	26.67	**8.60**	26.91	8.75
SARM	29.53	10.08	29.45	9.76	28.66	9.63	28.45	8.98
SARM-s	27.54	8.85	27.47	9.24	26.96	8.74	27.45	8.93
SARM-s-tuned	**26.95**	**8.72**	27.50	**8.90**	**26.53**	8.74	**26.46**	**8.65**

Table 3 reveals that while the performance of the "naive" SARM is not competitive, the results of SARM-s are only marginally inferior to those of the original VGGnets. We could alternatively treat SARM/SARM-s as the "pre-trained" version, and further tune it jointly with the classifier. The jointly-tuned SARM-s model, denoted as SARM-s-tuned, is able to achieve performance advantages over the original VGGnet. In "shallower" networks, the baseline models (ScatNet, PCANet, SARM) could often compete with, or even outperform the jointly-tuned networks (Stacked AE, FNN). From the imagenet experiments, we are reminded that the benefits of supervised fine-tuning become more evident, when the network goes deeper. In view of that, SARM could be potentially applied as an effective *pre-training* strategy for (very deep) DNNs.

Finally, it is worth noting that, while original VGG-16/19 models take around 10/12 days to train, with a single Titan X GPU and cuDNN v4, either SARM or SARM could be trained in hours. It takes 8 to 9 days to further tune SARM-s (for both VGG-16 and VGG-19 cases), which shows a 20%-25% accelerated convergence compared to training the original models from the scratch.

5.3 An Empirical Study of k-iteration ARM (k > 0) in SARM

In previous sections, we deal with SARMs consisting of only 0-iteration ARMs. We now introduce k-iteration ARM components with $k > 0$ to SARM, and carry out an empirical study on how it influences the performance. We choose the SARM of the VGG-19 architecture as the subject, and evaluate the top-5 classification errors under multi-scale testing. No joint tuning is performed.

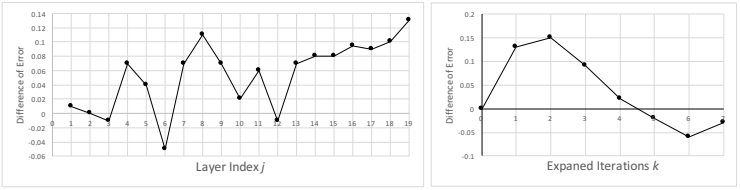

(a) (b)

Figure 3: The classification error differences of SARM, versus: (a) the index j of the ARM to be expanded for one more iteration; (b) the number of iterations k that the last ARM is expanded with.

Our first experiment is to "expand" the j-th ARM, which used to be 0-iteration, to become $k = 1$ iteration, following Eqns. (4) or (5), $j = 1, 2, \cdots, 19$. The differences[2] between the error rates of all the resulting 20-layer models, and that of the 19-layer SARM, are plotted in Fig. 3 (a). It is easy to observe that expanding an ARM, especially one of the last several, improves the overall performance of SARM. Given this observation, we carry out the second experiment to expand the last ARM ($j = 19$), for k more iterations, $k = 1, 2, \cdots, 7$. As plotted in Fig. 3 (b), while $k = 1, 2$ seems to benefit SARM most, a larger k could hurt its performance. We hypothesize that large k values will overly sparsify the input features and thus lose too much information, and plan to study it in future work.

6 Conclusion

We propose SARM, a simple yet powerful deep learning baseline, which can be obtained by solving a series of light-weight models. Extensive analyses and experiments given in this paper sufficiently conclude two facts: 1) SARM is easy to train, yet proves to be highly effective in extracting features for image classification tasks; 2) SARM serves as a valuable baseline, for studying advanced deep architectures. It also provides insights to the working mechanism of deep networks.

References

[1] T. Ahonen, A. Hadid, and M. Pietikainen. Face description with local binary patterns: Application to face recognition. *IEEE TPAMI*, 2006.
[2] Y. Bengio, P. Lamblin, D. Popovici, H. Larochelle, et al. Greedy layer-wise training of deep networks. *NIPS*, 2007.
[3] H. Bristow, A. Eriksson, and S. Lucey. Fast convolutional sparse coding. In *IEEE CVPR*, 2013.
[4] J. Bruna and S. Mallat. Invariant scattering convolution networks. *IEEE TPAMI*, 2013.
[5] T.-H. Chan, K. Jia, S. Gao, J. Lu, Z. Zeng, and Y. Ma. Pcanet: A simple deep learning baseline for image classification? *IEEE TIP*, 2015.
[6] A. Coates and A. Y. Ng. The importance of encoding versus training with sparse coding and vector quantization. In *ICML*, 2011.
[7] M. Elad and M. Aharon. Image denoising via sparse and redundant representations over learned dictionaries. *IEEE TIP*, 2006.
[8] K. Gregor and Y. LeCun. Learning fast approximations of sparse coding. In *ICML*, 2010.
[9] R. Gross, I. Matthews, J. Cohn, T. Kanade, and S. Baker. Multi-pie. *IVC*, 2010.
[10] K. He, X. Zhang, S. Ren, and J. Sun. Delving deep into rectifiers: Surpassing human-level performance on imagenet classification. In *IEEE ICCV*, 2015.
[11] K. He, X. Zhang, S. Ren, and J. Sun. Deep residual learning for image recognition. *IEEE CVPR*, 2016.
[12] K. He, X. Zhang, S. Ren, and J. Sun. Identity mappings in deep residual networks. *arXiv preprint arXiv:1603.05027*, 2016.
[13] S. Ioffe and C. Szegedy. Batch normalization: Accelerating deep network training by reducing internal covariate shift. *JMLR*, 2015.
[14] K. Jarrett, K. Kavukcuoglu, M. Ranzato, and Y. LeCun. What is the best multi-stage architecture for object recognition? In *IEEE CVPR*, 2009.
[15] Y. Jia, E. Shelhamer, J. Donahue, S. Karayev, J. Long, R. Girshick, S. Guadarrama, and T. Darrell. Caffe: Convolutional architecture for fast feature embedding. In *ACM MM*, 2014.

[2] A larger, positive difference means an improved performance compared to the SARM VGG-19 baseline.

[16] Z. Jiang, Z. Lin, and L. S. Davis. Learning a discriminative dictionary for sparse coding via label consistent k-svd. In *IEEE CVPR*, 2011.
[17] K. Kavukcuoglu, P. Sermanet, Y.-L. Boureau, K. Gregor, M. Mathieu, and Y. L. Cun. Learning convolutional feature hierarchies for visual recognition. In *NIPS*, 2010.
[18] A. Krizhevsky, I. Sutskever, and G. E. Hinton. Imagenet classification with deep convolutional neural networks. In *NIPS*, 2012.
[19] Y. LeCun, L. Bottou, Y. Bengio, and P. Haffner. Gradient-based learning applied to document recognition. *Proceedings of the IEEE*, 1998.
[20] C. Liu and H. Wechsler. Gabor feature based classification using the enhanced fisher linear discriminant model for face recognition. *IEEE TIP*, 2002.
[21] J. Long, E. Shelhamer, and T. Darrell. Fully convolutional networks for semantic segmentation. In *IEEE CVPR*, 2015.
[22] J. Masci, U. Meier, D. Cireşan, and J. Schmidhuber. Stacked convolutional auto-encoders for hierarchical feature extraction. In *ICANN*. 2011.
[23] R. Rubinstein, M. Zibulevsky, and M. Elad. Efficient implementation of the k-svd algorithm using batch orthogonal matching pursuit. *CS Technion*, 2008.
[24] K. Simonyan and A. Zisserman. Very deep convolutional networks for large-scale image recognition. *ICLR*, 2015.
[25] P. Sprechmann, A. Bronstein, and G. Sapiro. Learning efficient sparse and low rank models. *IEEE TPAMI*, 2015.
[26] I. Sutskever, J. Martens, G. Dahl, and G. Hinton. On the importance of initialization and momentum in deep learning. In *ICML*, 2013.
[27] Z. Wang, S. Chang, D. Liu, Q. Ling, and T. S. Huang. D3: Deep dual-domain based fast restoration of jpeg-compressed images. In *IEEE CVPR*, 2016.
[28] Z. Wang, S. Chang, J. Zhou, M. Wang, and T. S. Huang. Learning a task-specific deep architecture for clustering. *SDM*, 2016.
[29] Z. Wang, Q. Ling, and T. Huang. Learning deep ℓ_0 encoders. *AAAI*, 2016.
[30] Z. Wang, Y. Yang, S. Chang, Q. Ling, and T. S. Huang. Learning deep ℓ_∞ encoder for hashing. In *IJCAI*, 2016.
[31] B. Wen, S. Ravishankar, and Y. Bresler. Structured overcomplete sparsifying transform learning with convergence guarantees and applications. *IJCV*, 2015.
[32] B. Wohlberg. Efficient convolutional sparse coding. In *ICASSP*. IEEE, 2014.
[33] B. Xin, Y. Wang, W. Gao, and D. Wipf. Maximal sparsity with deep networks? *arXiv preprint arXiv:1605.01636*, 2016.
[34] C. Zhang, J. Liu, Q. Tian, C. Xu, H. Lu, and S. Ma. Image classification by non-negative sparse coding, low-rank and sparse decomposition. In *IEEE CVPR*, 2011.